BMC Oral Health

RESEARCH

Open Access

Chitosan nanogels enriched with granulocyte–macrophage colony-stimulating growth factor promote odontoblastic differentiation in human dental pulp stem cells in vitro

Bahar Asheghi[1], Khatereh Asadi[2,3], Ahmad Gholami[3,4,5], Maryam Enteghad[6], Seyedeh Saba Sadeghi[7] and Negin Firouzi[1*]

Abstract

Nanomaterials and regeneration-inducing microenvironments are key components of innovative regenerative endodontic treatment (RET). This study aimed to assess the odontogenic potential of granulocyte–macrophage colony-stimulating growth factor (GM-CSF) loaded chitosan nanogels (CNgs) on dental pulp stem cell (DPSCs) culture. GM-CSF/CNgs were prepared through the ionic gelation method and then characterized with Fourier transform infrared spectroscopy (FTIR), UV–visible spectrophotometry, dynamic light scattering (DLS), and zeta potential devices. Acridine orange (AO) and 4′,6-diamidino-2-phenylindole (DAPI) were used to evaluate cellular morphology and viability. The odontogenic and osteogenic differentiation was determined by quantitative real-time reverse-transcription PCR (qRT-PCR) and scanning electron microscopy (SEM). The physicochemical characterization confirmed that the GM-CSF/CNgs were prepared. The loading efficiency was 82.9 ± 2. Significant biocompatibility and no apparent nuclear fragmentation upon exposure to GM-CSF/CNgs and CNgs were observed. Quantifying the expression of dental pulp regeneration associated with genes including osteocalcin gene (OCN), dentin sialophosphoprotein (DSPP), and dentin matrix protein 1 (DMP1) between GM-CSF/CNgs and control groups was significant ($p < 0.001$). Morphology of DPSCs in contact with GM-CSF/CsNgs demonstrated odontogenic differentiation. GM-CSF/CNgs promoted a bioinspired drug delivery system (DDS) and induced dental pulp regeneration of DPSCs.

Keywords Chitosan Nanogels, Odontogenesis, Differentiation, Dental Pulp, Regeneration

*Correspondence:
Negin Firouzi
neginfirouzi@gmail.com
Full list of author information is available at the end of the article

Introduction

Regenerative endodontic treatments (RET) have been employed to mitigate the limitations of conventional apexification approaches for immature dental pulp necrosis and prolonged survival of permanent teeth [1]. Traditional RETs, including evoked-bleeding techniques, are ineffective for an extended range of dental diseases and often frustrating for clinicians and patients [2]. The innovative RET strategies focus on harnessing the nanomedicine potential to combine biomaterials, drugs, endogenous stem cells, and regeneration-inducing molecules to promote the repair, revascularization, and survival of dental pulp tissue and prevent bacterial infections. Thus, developing novel drug delivery systems (DDSs) based on RET is one unavoidable milestone to overcome the drawbacks [3, 4].

Nanomedicine, with the innovative design of natural nanostructures, revolutionized DDS products in the RET area [5]. Several investigations presented chitosan nanomaterial-based enhanced antimicrobial and osteoconductivity features [6–8]. Chitosan is constructed of glucosamine and N-acetylglucosamine components, with a significant resemblance to glycosaminoglycans (GAGs) of the extracellular matrix (ECM). Moreover, chitosan DDSs with unique properties such as biocompatibility, biodegradability, sterilization, antimicrobial, and immunomodulatory exhibit bioinspired microenvironments for osteogenic and odontogenic differentiation of dental pulp stem cells (DPSCs) [9–11]. When chitosan's advantages, combined with the unique features of nanogel structure, miniaturized hydrogel, and promising DDSs, were formed. In endodontics, chitosan nanogels (CNgs) displayed tremendous antimicrobial functions against the heterogeneity of fungi and bacterial strains [12, 13]. Furthermore, CNgs could be enriched with growth factors, drugs, and other revitalization agents, which required augmenting the DPSCs differentiation process [14, 15].

DPSCs exhibit multipotent mesenchymal stem cell properties with remarkable multi-lineage differentiation [16]. The proliferating and differentiating abilities of mesenchymal stem cells (MSCs) are determined via innate genetic programming, various immunoregulatory and signalling pathways, and external stimuli. Particularly, DPSCs with intrinsic properties could facilitate odontoblast replacement and dentin formation in injured dental tissue. These cells could secrete paracrine molecules to revitalize and revascularize necrotic tissue and promote dental pulp repair [17, 18].

Many studies have found that using a variety of growth factors and small molecules, such as vascular endothelial growth factor (VEGF), transforming growth factor β1 (TGF-β1), platelet-derived growth factor (PDGF), bone morphogenetic proteins (BMP-2), and a combination of several factors, to promote dental pulp regeneration [19–22]. Among them, granulocyte–macrophage colony-stimulating growth factor (GM-CSF) might be bioinspired for total dental pulp regeneration [23]. GM-CSF, also known as colony-stimulating factor 2 (CSF2), is a hematopoietic cytokine that enhances the count and function of leukocytes such as granulocytes, monocytes, and neutrophils [24, 25]. Few studies displayed that GM-CSF increased the blood supply of dental pulp tissue via revascularization and decreased apoptosis and inflammation [23]. GM-CSF.

Enhances the differentiation potential and homing ability of stem cells through ERK1/2- and/or PI3 K/Akt-signaling pathways [26]. It can be actively secreted in response to various injury signals and enhances the therapeutic capability of stem cells by promoting multi-lineage differentiation and migration. Furthermore, the increased expression of GM-CSF in the tissue fluid samples from radicular cystic lesions [27]. GM-CSF production may be closely related to an active state of inflammatory periradicular disease. Previous studies showed that G-CSF, as an inflammatory factor, mediated human periodontal ligament stem cells (hPDLSCs) proliferation and osteogenic differentiation. Given GM-CSF's ability to modulate the regenerative responses of stem cells, it may serve as a novel inductive factor to enhance odontogenic differentiation and the regenerative capacity of dental pulp stem cells (DPSCs) [28]. Furthermore, slight cytotoxicity was observed in the DPSCs culture treated with GM-CSF [29]. GM-CSF has a short half-life (~6 h), which leads to limited bioavailability and low stability throughout the body; its loading in CNgs might enhance cell uptake and remove alternative high-dose complications [30].

In the present study, we investigate the effect of GM-CSF-loaded CNgs in contact with DPSCs harvested cells. Nanostructures were synthesized and physicochemically characterized. The cell's morphology and live/dead assay were utilized to evaluate the biocompatibility. Dental pulp regeneration through electron microscopy, and osteogenic and odontogenic biomarkers expression were assessed in vitro.

Methods and materials

Materials

Chitosan (CAS-No 9012–76-4), tripolyphosphate (TPP, CAS-No 15091–98-2), GM-CSF (MDL number MFCD00166611), 4′,6-diamidino-2-phenylindole (DAPI) fluorescence (D9542), Acridine Orange (AO) solution

(A9231), Propidium iodide (PI) solution (P4864), and all chemical reagents were purchased from Sigma-Aldrich. RNA extraction kit (RiboEX reagent, GeneAll Biotechnology, Korea), Easy cDNA Synthesis Kit (Parstus, Iran), Master mix (Addbio, Korea), and Primers (sinaclon, Iran) were obtained.

Cell culture and identification

Human dental pulp-derived mesenchymal stem cells were sourced from the Iranian Biological Resource Center (IBRC code C10371). Low-glucose DMEM (Dulbecco's Modified Eagle Medium), fetal bovine serum (FBS), penicillin/streptomycin, trypsin–EDTA (0.25%), phosphate buffer saline (PBS) 1X, and other cell culture reagents were obtained from ATLAS Biologicals Colorado Company.

The hDPSCs were identified through surface markers and differentiation. The following fluorescent-conjugated antibodies were used to detect MSC cell surface markers at 4 °C for 30 min: IgG1-FITC as a negative control, CD90-RPE, CD105-RPE, CD45-FITC, CD34-RPE, and CD29-FITC (BD Pharmingen, San Diego, CA), which were visualized using flow cytometry (10MACSQuant, Miltenyi Biotec, Germany) and FlowJo 10.0 software (Flow Jo LLC, USA). For the differential induction, hDPSCs were cultured in lipogenic induction media containing 0.5 mM isobutylmethylxanthine, 1 mM dexamethasone, 10 mM insulin, and 0.2 mM indomethacin (all from Sigma-Aldrich) for 14 days and osteogenesis induction media containing 10 mM b-glycerophosphate, 50 mg/mL ascorbic acid, and 10 nM dexamethasone (all from Sigma-Aldrich) for 21 days, and subsequently stained with oil red O (Sigma-Aldrich) and alizarin red S (Sigma-Aldrich), respectively. Images were taken with an inverted optical microscope (Olympus Corporation, Tokyo, Japan) (S1).

GM-CSF/CNgs synthesis and characterization

CNgs are prepared through the ionic-gelation method, outlined by Asadi et al. [31–33]. Briefly, chitosan solution (2.0%, w/v) was prepared in an acetic acid aqueous solution (PH~4) and TPP as an ionic cross-linker prepared in distilled water. The concentration of TPP was three times that of the chitosan solution. The TPP solution was added to the chitosan solution in a stepwise manner under a magnetic stirrer at room temperature. After 30 min, the suspension was centrifuged at 10,000 ×g for 10 min. The supernatant was removed, and the deposited mass was resuspended in distilled water. For GM-CSF/CNgs preparation, the amount of GM-CSF (100 µmol/L) was combined with chitosan solution (0.2 mg/ml), then TPP added stepwise. The deposited mass resuspended at distilled water and supernatant contained unloaded GM-CSF.

GM-CSF/CNgs are characterized by Fourier transform infrared (FT-IR) spectroscopy (PerkinElmer, Spectrum RXI). The sample spectra were recorded in the context of KBr tablets in a range of over 4000–400 cm^{-1} at a resolution of 4 cm^{-1}. Dynamic light scattering (DLS) using a Malvern Zetasizer (ZEN 3600, UK) was applied to assess the size, hydrodynamic diameter, polydispersity index (PDI), and zeta potential. Finally, the morphology of prepared CNgs was evaluated by transmission electron microscopy (TEM, ZIESS, model EM10 C, Germany). The microstructure measurement software subsequently assessed the particle size analysis of CNgs.

Encapsulation efficiency

The standard curve ($R^2 = 0.99$) of GM-CSF was depicted via absorbance 280 nm of at least six concentrations using the UV-spectrophotometric (Cary 60 UV–Vis, China) method. The Encapsulation efficiency (EE) was calculated as follows Eqs. (1):

$$EE = \frac{\text{Total amount of GM} - \text{CSF} - \text{Free GM} - \text{CSF}}{\text{Total amount of GM} - \text{CSF}} \times 100 \quad (1)$$

Cell culture

Dental pulp stem cells (DPSCs) were harvested under high-glucose DMEM containing 10% fetal bovine serum (FBS) and 1% pen-strep, preserved in an incubator at 37 °C and 5% CO_2. When the cells were approximately 80% confluent, they were trypsinized and seeded into three groups of tissue culture dishes.

DPSCs with a density of 0.5 $\times 10^6$ cells/ml were exposed to GM-CSF/CNgs (2 mg/ml), CNgs (2 mg/ml), and control (without treatment) and then were used for in vitro examinations. The GM-CSF concentration was 100 µmol/L.

Cell morphology, viability with fluorescence microscopy

DPSCs were seeded on each tissue culture dish and treated with samples. The medium was removed, and then, a 10 nM DAPI stain solution was prepared and added according to a standardized protocol. After 20 min, the samples were washed 2–3 times in PBS, and the PBS and glycerol solution were added. Finally, the samples were evaluated with Olympus fluorescence microscopy (BX41, Japan).

For the AO study, an AO solution was prepared according to protocol guidelines, and 5 nM of the solution covered the DPSCs in each research group and was

preserved for 15 min at room temperature. Then, the cells were washed 2–3 times in PBS, and PI solution (1.0 mg/ml in PBS) was added to the samples. Finally, the DPSCs were washed in PBS and observed by Olympus fluorescence microscopy (BX41, Japan). Cells fluorescing green were scored as viable. Cells fluorescing orange, either fully or partially, were scored as nonviable. Image J software was used to analyze fluorescence microscopy results.

Cell morphology with scanning electron microscopy (SEM)

After 21 days, the morphology of DPSCs in contact with samples was evaluated by scanning electron microscopy (SEM, TESCAN, MIRA III, CZE). The samples were fixed in 2.5% glutaraldehyde solution for 1 h. The dehydration was done with a mixture of distilled water diluted with 70, 80, 90, and 100% alcohol for 15 min. Then, the samples were prepared and put on the SEM device.

Quantitative Real-Time PCR Analysis (qRT-PCR)

Samples were cultured in an osteogenic medium for 7 days and 21 days, and then the expression of osteo/odontogenic genes was analyzed with qRT-PCR. Each sample was extracted according to the RNA extraction kit protocol, and its quality was determined using the NanoDrop2000 spectrophotometer (Thermo Scientific, Waltham, MA, USA). In the next step, the Easy cDNA Synthesis Kit was used to synthesize cDNA, following the guidelines. The qRT-PCR method was performed with designed primers (Table 1) and according to the protocol of a high Rox Master Mix Green (2X) kit by Real-time PCR Thermocycler (ABI Stepone, USA). All the reactions processed under real-time cycles including initial denaturation (95 °C, 5 min), amplification in 40 times (95 °C for 15 s, 60 °C for 15–20 s, 72 °C for 15–30 s), melting curve (95 °C for 15 s, 65 °C for 1 min, and 65−−95 °C, slope: 0.3 °C/s), and cooling (30 °C for 20 s). All genes'threshold cycle (Ct) and melting curve were analyzed. The relative gene expression was determined via the comparative $2^{-\Delta\Delta CT}$ equation and normalized relative to GAPDH as the endogenous reference gene.

Table 1 Primer sequences for osteogenic, odontogenic biomarkers, and housekeeping genes employed in the study

Gene Name	Primer sequence (5´−3´)	Concentration
GAPDH	F: CTTTGGTATCGTGGAAGGAC R: GCAGGGATGATGTTCTGG	4 pmol/L
OCN	F: GGCAGCGAGGTAGTGAAGA R: GCAGAGCGACACCCTAGAC	4 pmol/L
DSPP	F:ATTTGGGCAGTAGCATGGG R:ATGCACCAGGACACCACTT	4 pmol/L
DMP1	F: TTCGTGAGAACATCCAGCC R: ACCCCGTTCACCTCATACT	4 pmol/L

Statistical analysis

All tests were performed in triplicate and in parallel independently ($n = 3$). The findings are presented as mean ± standard deviation (SD). Statistical analysis was performed using version 29.0 of the Statistical Package for Social Sciences. After confirming the data distribution's normality, a one-way analysis of variance (ANOVA) was performed, followed by Tukey's post-hoc test for comparisons between multiple groups. The criteria for statistical significance were set at $^{*}p < 0.05$, $^{**}p < 0.01$, and $^{***}p < 0.001$ for all group comparisons.

Results

GM-CSF/CNgs characterization

Size and zeta potential

The average hydrodynamic diameters of GM-CSF/CNgs and CNgs were 128.2 and 125.1 nm (Table 2) with a PDI~0.2. The Zeta potentials of GM-CSF/CNgs and CNgs are presented in Table 2, which shows that the synthesized samples have a surface charge of −1.1 mV and −1.17 mV, respectively. The result implies the colloidal stability of the prepared GM-CSF/CNgs.

The TEM images of GM-CSF/CNgs and (b) CNgs showed spherical morphology and uniform size distributions (Fig. 1). Moreover, particle size analysis showed GM-CSF/CNgs with 60.06 ± 6.78 nm (2a) and CNgs with 57.8 ± 8.8 nm (2b).

FT-IR The FT-IR spectra of CNgs and GM-CSF/CNgs are presented in Fig. 2. CNgs spectra showed 3400 cm^{-1}, corresponding to O–H stretching, and intramolecular hydrogen bonds. The polysaccharide characteristic peaks at 896 cm^{-1} and 1086 cm^{-1} belong to C-H symmetric and asymmetric stretching. The absorption band at 1617 cm^{-1} refers to the N–H bending of the amine group. The bands at 1220 cm^{-1}, 1160 cm^{-1}, 1100 cm^{-1}, and 875 cm^{-1} refer to P = O stretching, symmetric and antisymmetric stretching vibrations in the PO_2 group, symmetric and antisymmetric

Table 2 DLS (a) and zeta-potential of GM-CSF/CNgs and (b) CNgs

Samples	Particle diameter	PDI	Zeta potential
	4 h	4 h	4 h
CNgs	125.1	0.2	−0.1.1
GM-CSF/CNgs	128.2	0.2	−1.17

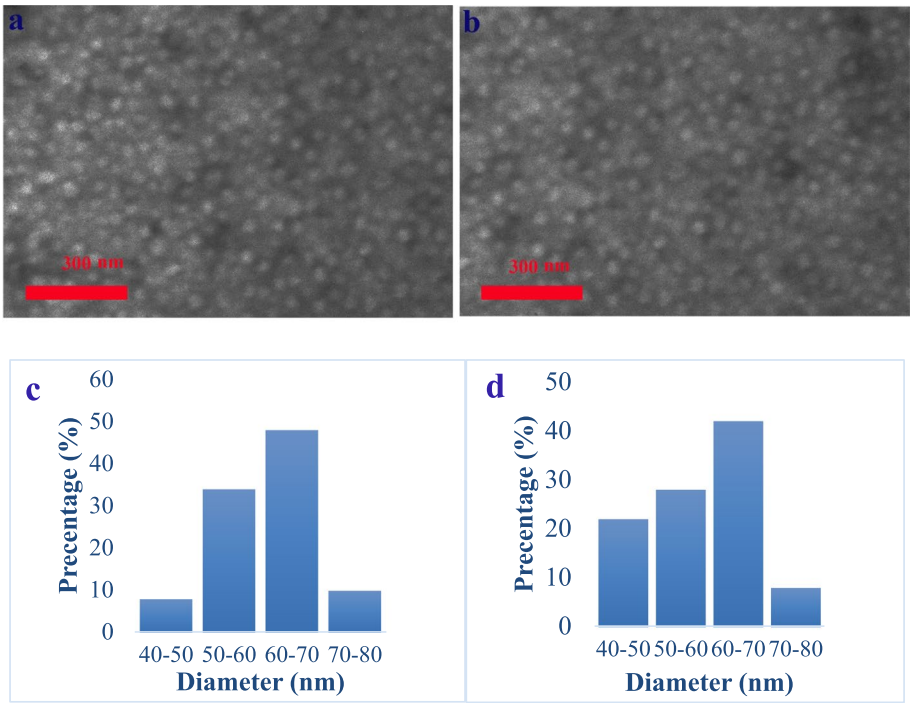

Fig. 1 TEM graph of (**a**) GM-CSF/CNgs and (**b**) CNgs; the size distribution of GM-CSF/CNgs (**c**) and CNgs (**d**)

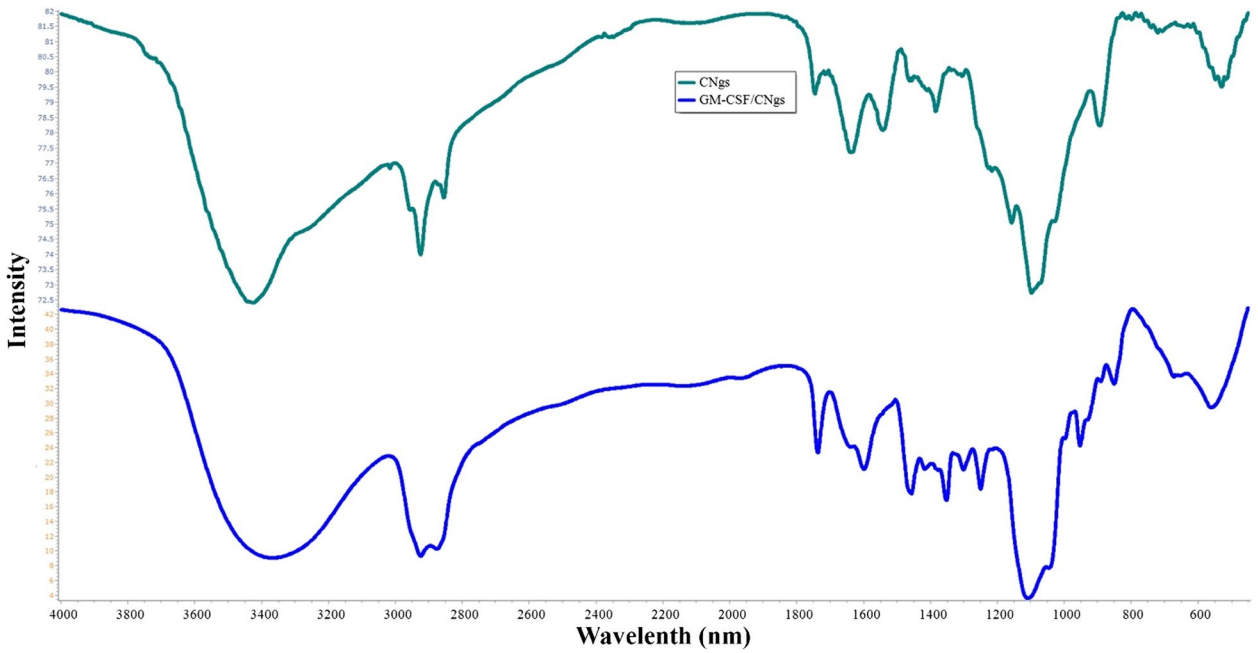

Fig. 2 the FT-IR spectra of GM-CSF/CNgs and CNgs

stretching vibrations in the PO_3 group, and antisymmetric stretching of the P-O-P bridge, respectively. The FT-IR of GM-CSF/CNgs showed the characteristic peaks of CNgs and the band related to the GM-CSF. The broad peaks at 3400 cm^{-1} belong to the N–H stretching of primary amine, and the peaks at 1614 cm^{-1} and 1667 cm^{-1} are associated with the C-N stretching of amide, respectively [34]. Therefore, the FT-IR spectra confirmed the spectral compatibility of the CNgs structure, and its comparison

with the GM-CSF/CNgs determined the formation of the intramolecular bonds of GM-CSF with CNgs.

Encapsulation efficiency

The drug EE of 82.9 ± 2% was obtained with no considerable effect on particle size.

Cell morphology and viability/adhesion of DPSCs exposed to GM-CSF/CNgs

After 72 h, the nuclear morphology of DPSCs treated with GM-CSF/CNgs and CNgs compared to the control was assessed by DAPI staining assay.

(Table 3). The DAPI images showed no obvious nuclear alteration (Fig. 3a). The quantitative results showed

Table 3 Results of the DAPI staining assay showing the viability and adhesion of DPSCs treated with GM-CSF/CNgs and CNgs compared to the control

Number of nuclei/mm^2		Mean	Std. Deviation	*P* value
Grouped by materials	Control	398.0 a	19.70	**0.1979 (ns)**
	Nanohydrogel	350.0 a	36.06	
	GMCSF + Nanohydrogel	383.7 a	29.26	

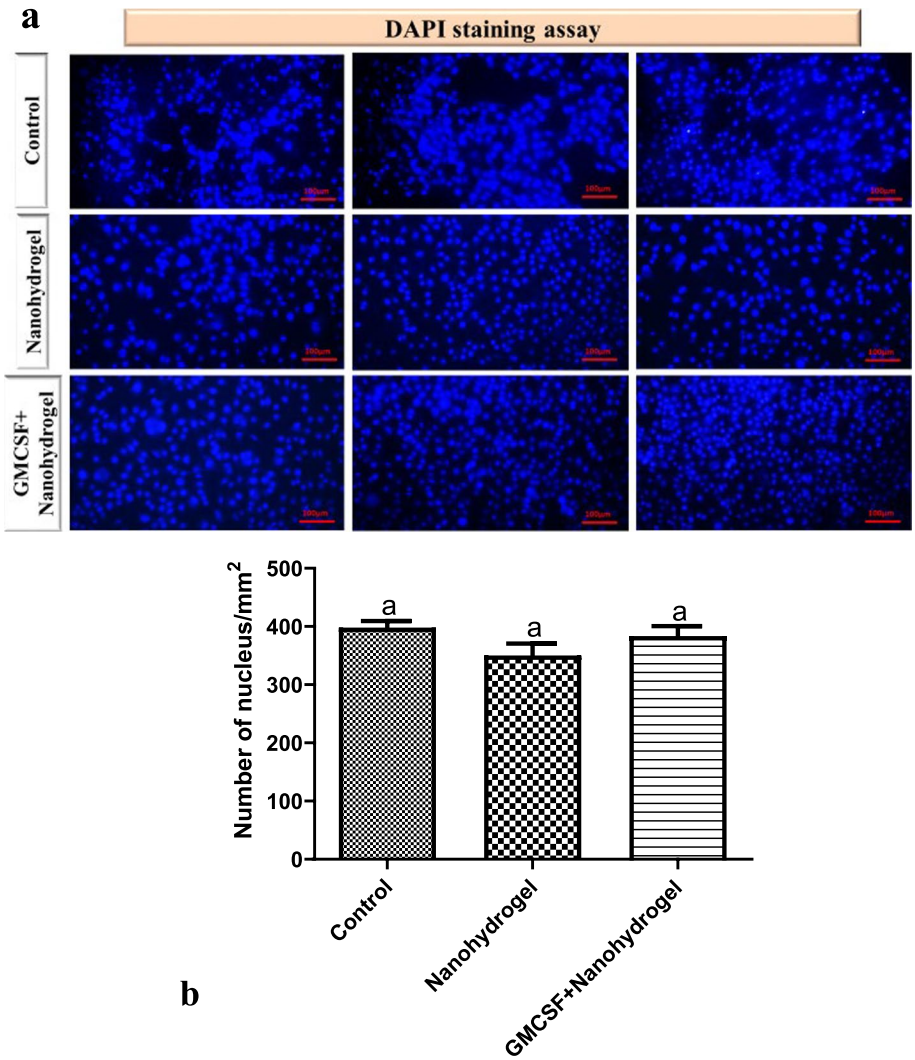

Fig. 3 Fluorescence microscopic images of DPSCs treated with GM-CSF/CNgs and CNgs compared to the control group (without treatment) with DAPI staining (**a**), the number of nucleus/mm.^{2} between all the groups of study (**b**)

no significant differences in cell viability, apoptosis, or nuclear fragmentation among all groups (Fig. 3b).

After 7 days of DPSCs treated with GM-CSF/CNgs and CNgs compared to the control group. The AO = PI staining (Fig. 4) illustrated significant biocompatibility and cell viability (%) between treated cells compared to the control. Furthermore, almost all the DPSCs in treated and control groups emit green fluorescence in the context of AO/PI staining that determined are live cells (Fig. 4a). Besides, the quantitative analysis (Table 4) confirmed the biocompatibility.

Expression of odontogenic and odontogenic differentiation genes of DPSCs exposed to GM-CSF/CsNg

After 21 days, the results obtained from qRT-PCR showed the expression of odontogenic associating genes, including dentin sialophosphoprotein (DSPP) and dentin matrix protein 1 (DMP1) between GM-CSF/CNgs and control groups were significant ($p < 0.001$), and also these genes expression were significant among CNgs and control groups ($p < 0.05$) (Fig. 5a, 5b). Furthermore, the osteogenic biomarker osteocalcin (OCN) higher expression

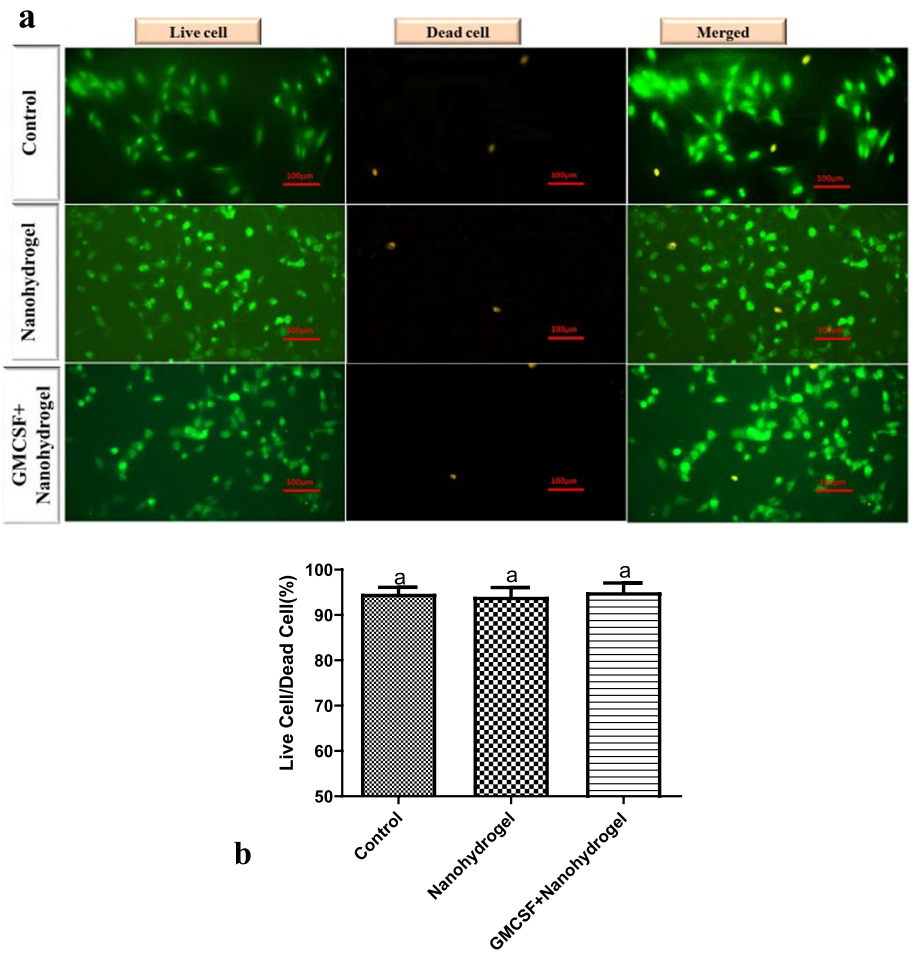

Fig. 4 Fluorescence microscopic images of DPSCs treated with GM-CSF/CNgs and CNgs compared to the control group (without treatment) with AO-PI staining (**a**), the percentages of live/dead cells between all the groups of study (**b**)

Table 4 Acridine orange staining assay results showing the percentage of live DPSCs to dead DPSCs treated with GM-CSF/CNgs and CNgs compared to control

Live cells/dead cells (%)		Mean	Std. Deviation	*P* value
Grouped by materials	Control	94.67 a	2.517	0.9312 (ns)
	Nanohydrogel	94.00 a	3.606	
	GMCSF + Nanohydrogel	95.00 a	3.606	

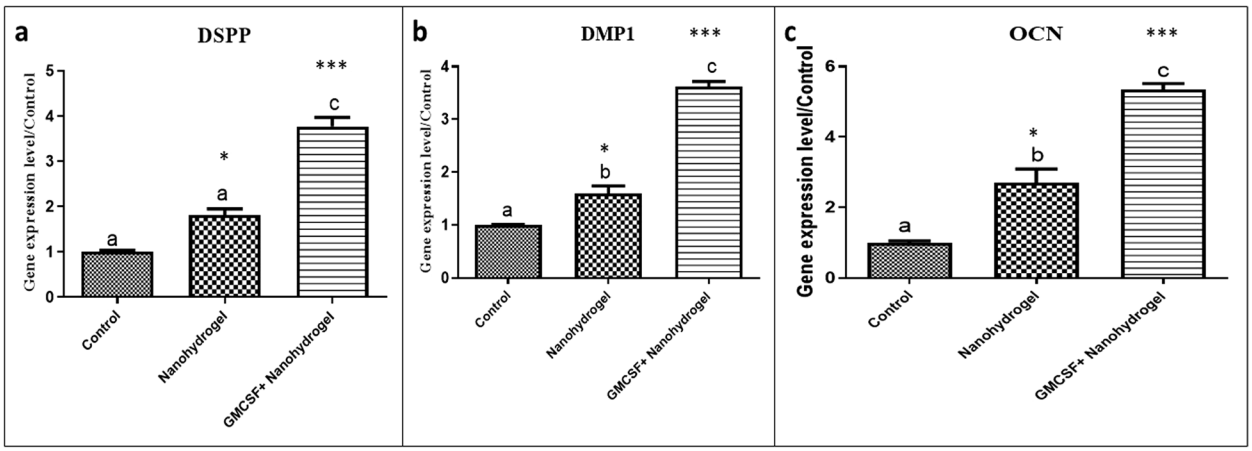

Fig. 5 Gene expression profile of DPSCs treated with GM-CSF/CNgs and CNgs compared to the control group (without treatment) on day 21. Rest software was used for gene expression analysis using real-time PCR data. A statistical significance was indicated with asterisks (***$p < 0.001$, *$p < 0.05$)

was observed in GM-CSF/CNgs ($p < 0.001$) and CNgs ($p < 0.05$) compared to control (Fig. 5c).

Cell morphology of DPSCs exposed to GM-CSF/CNg

After 21 days, SEM observation exhibited morphological changes in DPSCs exposed to CNgs (Fig. 6a) and GM-CSF/CNgs (Fig. 6b). The morphology of DPSCs exposed to GM-CSF/CNgs demonstrated spindle-shaped fibroblast-like cell morphology, mineralization of the intracellular matrix, and elongation of cytoplasmic processes, indicating cell adhesion and interactions with the surface of CNgs and GM-CSF/CNgs.

Discussion

In the present study, we attempted to synthesize GM-CSF-loaded CNgs and assessed the potential of DPSCs treated with them in dental pulp regeneration. Characterization methods, including FTIR, DLS, and Zeta potential, confirmed GM-CSF/CNgs formation. The cellular staining and q-RT PCR results demonstrate that GM-CSF/CNgs provided a biocompatible substrate for inducing dental pulp differentiation of DPSC culture.

Long-term teeth survival, preserving the function of the dental pulp, and restoring infected permanent immature teeth required novel RET procedures to replace injured and necrotic dental tissue with newborn tissue [35]. Literature reveals that in the context of the notable resemblance to the ECM physicochemical features, chitosan hydrogels in exposure to DPSCs improved viability, adhesion, proliferation, and osteogenic or odontogenic differentiation [5, 7, 36]. Besides, we approved the noteworthy antibacterial performance, antioxidant activity, negligible cytotoxicity effect, and potent therapeutic potential on mucositis ulcers of CNgs in further studies, which could be helpful in endodontic pro-regenerative space sterilization [31, 33]. According to the results of our research, DPSCs treated with GM-CSF/CNgs and CNgs showed minimal cell retention, cell death, and

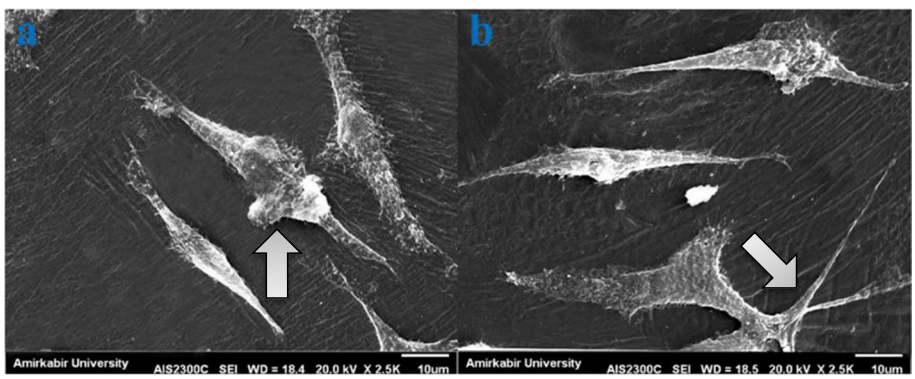

Fig. 6 SEM images of DPSCs differentiated on CNgs show a typical odontoblast-like morphology, compaction, and mineralization of the intracellular matrix (arrow) (**a**). GM-CSF/CNgs – cellular cytoplasmic extensions adhering to nanohydrogels (arrow) (**b**)

significant cell viability (Fig. 4). Furthermore, no apparent nuclear fragmentation of GM-CSF/CNgs and CNgs was observed (Fig. 3). Moreover, CNgs enriched with GM-CSF/CNgs exhibited synergistic proliferative effects compared to CNgs. Although there are no significant differences between GM-CSF/CNgs and CNgs with control groups, it should be considered that GM-CSF could activate proliferation mechanisms, leading to the slight increase in GM-CSF/CNgs compared to CNgs-treated groups. It was previously suggested that GM-CSF could stimulate the mobilization and proliferation of DPSCs [34, 37, 38].

The dental pulp is a complex of odontoblasts, connective tissue, blood vessels, and neural tissue encased by dentin tissue. GM-CSF is a hematopoietic growth factor that could induce neovasculature formation, and its potential in neural tissue regeneration has been approved previously [39–41]. Moreover, chitosan nanocarriers could stimulate the migration and proliferation of vascular endothelial cells to facilitate angiogenesis, increase blood supply, and microvessel density [42].

However, the odontogenic effects of GM-CSF were under debate. The results of the present study suggest that a 100 µmol/L concentration of GM-CSF loaded in CNgs provoked odontogenic differentiation of DPSCs. The characteristic odontogenic markers DSPP and DMP1 expression were higher in GM-CSF/CNgs than in the blank control group (Fig. 5). Interestingly, it was similarly expressed in DPSCs in contact with CNgs, although it is lower than that from GM-CSF/CNgs ($p < 0.05$); this may be due to the porous 3D structure, which is ideal for cell adhesion and proliferation. Our results are inconsistent with Altari et al.'s finding that dental pulp stem cells (DPSCs) cultured on chitosan scaffolds, with or without TGF-b1, showed mineral deposition and odontogenic differentiation.[43] Literature reports have confirmed that the DSPP and DMP1 play crucial roles during the stages of dental pulp development to specify odontoblastic differentiation, and could also be helpful in late dentin mineralization [44]. Furthermore, DSPP increased the production of dentin sialoprotein (DSP) and dentin phosphoprotein (DPP), which are essential factors in the dentinogenesis process [45]. K Iohara et al. reported that aGM-CSF plays a key role in total dental pulp regeneration. There was a significant amount of regenerated dentin-pulp complex, cell migration, neurite outgrowth, and reduced inflammatory cues or apoptotic components [23]. In this study, there was a higher expression of the early osteogenic marker OCN in the groups exposed to the treatments compared to the control. However, it showed a significant increase in DPSCs in contact with GM-CSF/CNgs (Fig. 5c). The OCN is found in dentin mineralized matrix and regulates the mineral nodule formation in normal teeth's hard tissue development [46]. DSPP, DMP1, and OCN biomarker expression are directly involved in dental pulp morphogenesis and regeneration of injured tissues. Thus, GM-CSF/CNgs exhibited potential for higher efficiency in generating dental pulp. In addition, morphological alteration and calcified deposition could be observed in DPSCs in contact with the treatments in SEM micrographs (Fig. 6). Within the study's limitations, it can be concluded that GM-CSF-loaded chitosan nanohydrogel, by modulating the microenvironment, serves as a suitable injectable scaffold enriched with growth factors and cytokines that promote odontogenic differentiation pathways through the sustained release of GM-CSF within the root canal. This targeted stimulation results in a more predictable, biologically driven alternative regenerative endodontic treatment than traditional methods, aimed at preserving tooth vitality and function.

Conclusions

The present study displayed a bioinspired drug delivery system (DDS) for inducing dental pulp regeneration of DPSCs treated with GM-CSF/CNgs. However, further studies must be performed to assess other vital characteristics of GM-CSF/CNgs, such as angiogenesis, neurogenesis properties, and anti-inflammatory features for clinical translation.

Abbreviations

GM-CSF	Granulocyte-Macrophage Colony-Stimulating Factor
CNgs	Chitosan Nanogels
DPSCs	Dental Pulp Stem Cells
DMEM	Dulbecco's Modified Eagle Medium
FBS	Fetal Bovine Serum
qRT-PCR	Quantitative Real-Time Reverse Transcription PCR
DAPI	4',6-Diamidino-2-Phenylindole
AO	Acridine Orange
PI	Propidium Iodide
SEM	Scanning Electron Microscopy
TEM	Transmission Electron Microscopy
FTIR	Fourier Transform Infrared Spectroscopy
PBS	Phosphate Buffered Saline
OCN	Osteocalcin
DSPP	Dentin Sialophosphoprotein
DMP1	Dentin Matrix Protein 1
PDI	Polydispersity Index
TPP	Tripolyphosphate
RET	Regenerative Endodontic Treatment

Supplementary Information

The online version contains supplementary material available at https://doi.org/10.1186/s12903-025-06185-x.

Supplementary Material 1.

Acknowledgements
The authors of this paper would like to appreciate the Vice-Chancellery of Shiraz University of Medical Science for supporting this study.

Authors' contributions
BA and AGH carried out the literature research, participated in its design and coordination, and supervised the writing of the manuscript. NF and KA fulfilled the investigations, wrote the manuscript, and prepared the figures for the study. SSS and ME contributed to data collection and analysis. All authors read and approved the final manuscript.

Funding
Not applicable.

Data availability
Data will be provided by authors upon request from editorial board.

Declarations

Ethics approval and consent to participate
This study was approved by the Research Ethics Committee of Shiraz University of Medical Science with approval number Ethics Committee Approval: #IR.SUMS.REC.1402.437. Informed consent was obtained from all participants.

Consent for publication
Consent for publication was obtained from all participants in the current study.

Competing interests
The authors declare no competing interests.

Author details
[1]Department of Endodontics, School of Dentistry, Shiraz University of Medical Sciences, Ghasrodasht St, Mehr Ave, Shiraz 71956–15878, Iran. [2]Guilan Road Trauma Research Center, Trauma Institute, Guilan University of Medical Sciences, Rasht, Iran. [3]Biotechnology Research Center, Shiraz University of Medical Sciences, Shiraz, Iran. [4]Department of Medical Nanotechnology, School of Advanced Medical Science and Technology, Shiraz University of Medical Sciences, Shiraz, Iran. [5]Department of Pharmaceutical Biotechnology, School of Pharmacy, Shiraz University of Medical Sciences, Shiraz, Iran. [6]Department of Endodontics, School of Dentistry, Isfahan University of Medical Sciences, Isfahan, Iran. [7]Student Research Committee, School of Dentistry, Shiraz University of Medical Sciences, Shiraz, Iran.

Received: 27 July 2024 Accepted: 16 May 2025
Published online: 01 July 2025

References

1. Alghamdi FT, Alqurashi AE. Regenerative Endodontic Therapy in the Management of Immature Necrotic Permanent Dentition: A Systematic Review. TheScientificWorldJOURNAL. 2020;2020:7954357.
2. Mao JJ, Kim SG, Zhou J, Ye L, Cho S, Suzuki T, et al. Regenerative endodontics: barriers and strategies for clinical translation. Dent Clin North Am. 2012;56(3):639–49.
3. Thant AA, Ruangpornvisuti V, Sangvanich P, Banlunara W, Limcharoen B, Thunyakitpisal P. Characterization of a bioscaffold containing polysaccharide acemannan and native collagen for pulp tissue regeneration. Int J Biol Macromol. 2023;225:286–97.
4. Gholami A, Asadi K, Samiraninezhad N, Ghaffaripour D, Safari A, Ghahramani Y, Abbaszadegan A. Triple antibiotic paste versus nano calcium hydroxide as an intracanal medicament in human primary molars: a randomized clinical trial. Giornale Italiano di Endodonzia. 2023;35.
5. Samiraninezhad N, Asadi K, Rezazadeh H, Gholami A. Using chitosan, hyaluronic acid, alginate, and gelatin-based smart biological hydrogels for drug delivery in oral mucosal lesions: A review. Int J Biol Macromol. 2023;252: 126573.
6. Hoveizi E, Naddaf H, Ahmadianfar S, Gutmann JL. Encapsulation of human endometrial stem cells in chitosan hydrogel containing titanium oxide nanoparticles for dental pulp repair and tissue regeneration in male Wistar rats. J Biosci Bioeng. 2023;135(4):331–40.
7. Gholami A, Rahmanian A, Mirzaei E, Mozaffariyan F, Asadi K, Omidifar N. Vancomycin coupled chitosan/PEO nanofibrous scaffold with the desired antibacterial activity as a potential for biomedical application. Journal of Bioactive and Compatible Polymers.0(0):08839115231195796.
8. Gholami A, Ghezelbash K, Asheghi B, Abbaszadegan A, Amini A. An In Vitro Study on the Antibacterial Effects of Chlorhexidine-Loaded Positively Charged Silver Nanoparticles on Enterococcus faecalis. J Nanomater. 2022;2022:6405772.
9. Kim JE, Park S, Lee W-S, Han J, Lim JW, Jeong S, et al. Enhanced Osteogenesis of Dental Pulp Stem Cells In Vitro Induced by Chitosan–PEG-Incorporated Calcium Phosphate Cement. Polymers. 2021;13(14):2252.
10. Bakopoulou A, Georgopoulou **A**, Grivas I, Bekiari C, Prymak O, Loza **K**, et al. Dental pulp stem cells in chitosan/gelatin scaffolds for enhanced orofacial bone regeneration. Dental materials : official publication of the Academy of Dental Materials. 2019;35(2):310–27.
11. Eskandari F, Mofidi H, Asheghi B, Mohammadi F, Gholami A. Bringing resistance modulation to methicillin-resistant Staphylococcus aureus (MRSA) and vancomycin-resistant enterococci (VRE) strains using a quaternary ammonium compound coupled with zinc oxide nanoparticles. World J Microbiol Biotechnol. 2023;39(7):193.
12. Alhomrany R, Zhang C, Chou L. Cytotoxic effect of chitosan nanoparticles on normal human dental pulp cells. Nanoscience and Nanotechnology. 2019;3(1).
13. Karimi Z, Asadi K, Ghahramani P, Gholami A. Trinitroglycerine-loaded chitosan nanoparticles attenuate renal ischemia-reperfusion injury by modulating oxidative stress. Sci Rep. 2024;14(1):32112.
14. Wu S, Zhou Y, Yu Y, Zhou X, Du W, Wan M, et al. Evaluation of chitosan hydrogel for sustained delivery of VEGF for odontogenic differentiation of dental pulp stem cells. Stem cells international. 2019;2019.
15. Ducret M, Montembault A, Josse J, Pasdeloup M, Celle A, Benchrih R, et al. Design and characterization of a chitosan-enriched fibrin hydrogel for human dental pulp regeneration. Dent Mater. 2019;35(4):523–33.
16. Labedz-Maslowska A, Bryniarska N, Kubiak A, Kaczmarzyk T, Sekula-Stryjewska M, Noga S, et al. Multilineage Differentiation Potential of Human Dental Pulp Stem Cells-Impact of 3D and Hypoxic Environment on Osteogenesis In Vitro. International journal of molecular sciences. 2020;21(17).
17. Firouzi N, Yavari HR, Rahimi S, Roshangar L, Chitsazha R, Amini M. Concentrated Growth Factors Combined with Lipopolysaccharide Stimulate the In Vitro Regenerative and Osteogenic Activities of Human Dental Pulp Stem Cells by Balancing Inflammation. International journal of dentistry. 2022;2022:2316666.
18. Mattei V, Martellucci S, Pulcini F, Santilli F, Sorice M, Delle MS. Regenerative Potential of DPSCs and Revascularization: Direct, Paracrine or Autocrine Effect? Stem cell reviews and reports. 2021;17(5):1635–46.
19. Divband B, Aghazadeh M, Al-Qaim ZH, Samiei M, Hussein FH, Shaabani A, et al. Bioactive chitosan biguanidine-based injectable hydrogels as a novel BMP-2 and VEGF carrier for osteogenesis of dental pulp stem cells. Carbohyd Polym. 2021;273: 118589.
20. Divband B, Pouya B, Hassanpour M, Alipour M, Salehi R, Rahbarghazi R, et al. Towards Induction of Angiogenesis in Dental Pulp Stem Cells Using Chitosan-Based Hydrogels Releasing Basic Fibroblast Growth Factor. Biomed Res Int. 2022;2022:5401461.
21. Jiang L, Ayre WN, Melling GE, Song B, Wei X, Sloan AJ, Chen X. Liposomes loaded with transforming growth factor β1 promote odontogenic differentiation of dental pulp stem cells. J Dent. 2020;103: 103501.
22. Zhang M, Jiang F, Zhang X, Wang S, Jin Y, Zhang W, Jiang X. The Effects of Platelet-Derived Growth Factor-BB on Human Dental Pulp Stem Cells Mediated Dentin-Pulp Complex Regeneration. Stem Cells Transl Med. 2017;6(12):2126–34.
23. Iohara K, Murakami M, Takeuchi N, Osako Y, Ito M, Ishizaka R, et al. A novel combinatorial therapy with pulp stem cells and granulocyte colony-stimulating factor for total pulp regeneration. Stem Cells Transl Med. 2013;2(7):521–33.
24. Raj AT, Kheur S, Khurshid Z, Sayed ME, Mugri MH, Almasri MA, et al. The Growth Factors and Cytokines of Dental Pulp Mesenchymal Stem Cell

Secretome May Potentially Aid in Oral Cancer Proliferation. Molecules. 2021;26(18):5683.
25. Nakayama H, Iohara K, Hayashi Y, Okuwa Y, Kurita K, Nakashima M. Enhanced regeneration potential of mobilized dental pulp stem cells from immature teeth. Oral Dis. 2017;23(5):620–8.
26. Park S-R, Cho A, Kim J-W, Lee H-Y, Hong I-S. A Novel Endogenous Damage Signal, CSF-2, Activates Multiple Beneficial Functions of Adipose Tissue-Derived Mesenchymal Stem Cells. Mol Ther. 2019;27(6):1087–100.
27. Chen Y, Zhou M, Liu J, Chi J, Yang X, Du Q, et al. Multiple effects of dose-related GM-CSF on periodontal resorption in deep-frozen grafted teeth: A reverse study. Int Immunopharmacol. 2024;130: 111745.
28. Gervásio AM, Silva DAO, Taketomi EA, Souza CJA, Sung S-SJ, Loyola AM. Levels of GM-CSF, IL-3, and IL-6 in Fluid and Tissue from Human Radicular Cysts. Journal of Dental Research. 2002;81(1):64–8.
29. Jenkner S. Enhancing Dental Pulp Stem Cell Viability for Treatment of Spinal Cord Injury via Immune Cell Preconditioning 2020.
30. Yeapuri P, Olson KE, Lu Y, Abdelmoaty MM, Namminga KL, Markovic M, et al. Development of an extended half-life GM-CSF fusion protein for Parkinson's disease. Journal of controlled release : official journal of the Controlled Release Society. 2022;348:951–65.
31. Khatereh Asadi RH, Mohammad Mehdi Ommati, Mehrdad Hamidi, Shahrokh Yousefzadeh-Chabok, Nazafarin Samiraninezhad, Mehdi Khoshneviszadeh, Masoud Hashemzaei, Ahmad Gholami. Nitroglycerin-Loaded Chitosan Nanogels: Shedding Light on Cytotoxicity, Antioxidativity, and Antibacterial Activities biomateria r. 2023.
32. Asadi K, Azarpira N, Heidari R, Hamidi M, Yousefzadeh-Chabok S, Nemati MM, et al. Trinitroglycerin-loaded chitosan nanogels accelerate angiogenesis in wound healing process. Int J Biol Macromol. 2024;278: 134937.
33. Samiraninezhad N, Asadi K, Heidari R, Rezaee M, Gholami A, Amini A. Development of a doxepin-loaded chitosan nanogel as an innovative nano platform for oral mucositis treatment. Journal of Drug Delivery Science and Technology. 2025;104: 106430.
34. Dehkordi N, Minaiyan M, Talebi A, Akbari V, Taheri A. Nanocrystalline cellulose–hyaluronic acid composite enriched with GM-CSF loaded chitosan nanoparticles for enhanced wound healing. Biomedical Materials. 2019;14.
35. Ribeiro JS, Sanz CK, Münchow EA, Kalra N, Dubey N, Suárez CEC, et al. Photocrosslinkable methacrylated gelatin hydrogel as a cell-friendly injectable delivery system for chlorhexidine in regenerative endodontics. Dent Mater. 2022;38(9):1507–17.
36. Moreira MS, Sarra G, Carvalho GL, Gonçalves F, Caballero-Flores HV, Pedroni ACF, et al. Physical and Biological Properties of a Chitosan Hydrogel Scaffold Associated to Photobiomodulation Therapy for Dental Pulp Regeneration: An In Vitro and In Vivo Study. Biomed Res Int. 2021;2021:6684667.
37. Kim J, Kim NK, Park SR, Choi BH. GM-CSF Enhances Mobilization of Bone Marrow Mesenchymal Stem Cells via a CXCR4-Medicated Mechanism. Tissue Engineering and Regenerative Medicine. 2019;16(1):59–68.
38. Murakami M, Horibe H, Iohara K, Hayashi Y, Osako Y, Takei Y, et al. The use of granulocyte-colony stimulating factor induced mobilization for isolation of dental pulp stem cells with high regenerative potential. Biomaterials. 2013;34(36):9036–47.
39. Kovacic JC, Muller DWM, Graham RM. Actions and therapeutic potential of G-CSF and GM-CSF in cardiovascular disease. J Mol Cell Cardiol. 2007;42(1):19–33.
40. Bhattacharya P, Thiruppathi M, Elshabrawy HA, Alharshawi K, Kumar P, Prabhakar BS. GM-CSF: An immune modulatory cytokine that can suppress autoimmunity. Cytokine. 2015;75(2):261–71.
41. Wallner S, Peters S, Pitzer C, Resch H, Bogdahn U, Schneider A. The Granulocyte-colony stimulating factor has a dual role in neuronal and vascular plasticity. Frontiers in Cell and Developmental Biology. 2015;3.
42. Sadeghi A, Moztarzadeh F, Aghazadeh MJ. Investigating the effect of chitosan on hydrophilicity and bioactivity of conductive electrospun composite scaffold for neural tissue engineering. Int J Biol Macromol. 2019;121:625–32.
43. Altairi AMR, El-sherbiny I, Elhindawy M, yahia s, badr a. Effects of 3D Chitosan nanofibrous scaffold and TGFβ1 on Dental pulp stem cells (DPSCs) differentiation. Egyptian Dental Journal. 2023;69(3):2351–8.
44. Guo S, Lim D, Dong Z, Saunders TL, Ma PX, Marcelo CL, Ritchie HH. Dentin Sialophosphoprotein: A Regulatory Protein for Dental Pulp Stem Cell Identity and Fate. Stem Cells and Development. 2014;23(23):2883–94.
45. Chaussain C, Eapen AS, Huet E, Floris C, Ravindran S, Hao J, et al. MMP2-cleavage of DMP1 generates a bioactive peptide promoting differentiation of dental pulp stem/progenitor cells. Eur Cell Mater. 2009;18:84–95.
46. Mortada I, Mortada R. Dental pulp stem cells and osteogenesis: an update. Cytotechnology. 2018;70(5):1479–86.

Publisher's Note